20.3dB 0.39mW AM Detector with Single-Transistor Active Inductor in Bendable a-IGZO TFT

Tilo Meister*, Koichi Ishida*, Reza Shabanpour*, Bahman K.-Boroujeni*, Corrado Carta*, Niko Münzenrieder[†‡], Luisa Petti[†], Giuseppe Cantarella[†], Giovanni A. Salvatore[†], Gerhard Tröster[†], Frank Ellinger*

*Faculty of Electrical and Computer Engineering, Technische Universität Dresden, Dresden, Germany

[†]Electronics Laboratory, Swiss Federal Institute of Technology Zurich, Zurich, Switzerland

[‡]Sensor Technology Research Center, School of Engineering and Informatics, University of Sussex, United Kingdom

***Abstract*—This paper presents an AM detector circuit in a bendable a-IGZO TFT technology. The circuit is based on a common-source stage loaded with a single-ended active inductor, which uses only one active transistor. This active inductor is the key element for the achieved circuit performance. The detector circuit consumes only 0.39 mW, which is almost a tenfold improvement over previous works in the same technology and crucial for mobile and wearable applications. At the same time it has the smallest chip area. The detector provides a conversion gain of 20.3 dB and an RF -3dB-bandwidth of around 7.5 MHz. At fc=13.56 MHz it has 11.6 dB gain, which also allows its use in this unlicensed ISM radio band for RFID and smart label applications.**

Keywords—flexible electronics; radio receivers; amplifiers; active inductors; thin film transistors; TFT; amplitude modulation; a-IGZO; InGaZnO

I. INTRODUCTION

With the recent progress made in the operation frequency of flexible thin-film and large area electronics its potential for applications is studied extensively. One crucial functionality for many applications is power efficient wireless communication [1]. For this purpose, we present an AM detector in a fully flexible amorphous Indium-Gallium-Zinc-Oxide (a-IGZO) thin-film transistor (TFT) technology [2]. It is one of the most promising materials for flexible electronics, because of its high field-effect mobility of more than 10 cm²/Vs. Furthermore, a-IGZO TFT circuits can be fabricated at low temperatures and on flexible substrates such as Polyimide [3].

However, this technology has limitations, which impose circuit design constraints. Prominent ones are that it only has n-type transistors, cannot implement on-chip inductors, and does not provide a dedicated resistive layer. Flexible inductors in thin film technology are in general a challenge, because their inductance depends on their bending radius. Also, they require a large area and achieve only limited quality factors due to the comparably high parasitic resistance and capacitances, which result directly from the small layer thicknesses.

We aim at implementing a fully flexible smart label that can receive a low data rate on-off keying (OOK) signal to trigger events and actuators. For this purpose we target a low power consumption, high gain, and small chip area, while linearity is a secondary concern. The baseband frequency f_{bb} range is targeted to be wide and in the low kHz-range. The carrier frequency f_c is targeted to be above 1 MHz. As mentioned above, an inductor, which conventionally can provide very good electrical performance, cannot be used in fully flexible thin film electronics. Instead the key element in this work is the innovative realization of an active single-ended inductor with only one active transistor in TFT technology, which is used as active load to a common-source (CS) amplifier stage. The presented active inductor has a low complexity and requires only a small chip area, because it is based on only one active transistor, a capacitor, and a resistance. By this means we reach the target performance in a fully integrated, fully flexible circuit.

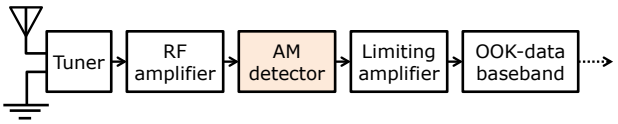

Fig. 1. System structure of targeted OOK receiver modul for smart labels excluding triggered events and actuators on the right side.

II. SYSTEM OVERVIEW

The presented circuit realizes AM detection, i.e. envelope detection, by half-wave rectification and low-pass filtering. It is optimized for use in an OOK data receiver module of a smart label. The system structure is outlined in Fig. 1. To realize the full receiver module, we individually implement the functional blocks shown in Fig. 1 as circuits in a-IGZO TFT technology [2] (variant with a gate to source/drain overlap L_{OV} of 5 µm). The circuit blocks are intended to be packaged into a complete receiver module and smart label. The tuner circuit as well as the packaging technology are described in [4]; an antenna is described in [5]; RF amplifier circuits are presented in [6, 7]. As mentioned above, the primary optimization goals for this AM detector circuit are gain/sensitivity, power consumption, and area, while linearity is of secondary importance in this digital application. For these goals we introduce a single-ended active inductor of low complexity and small area.

III. AM DETECTOR CIRCUIT

A. Schematic and Basic Principle

The full schematic as well as a simplified schematic of the presented AM detector circuit are shown in Fig. 2 and Table I. AM detection and gain are provided by the CS stage consisting of saturated M1 and the single-ended active inductor circuit Z3. Transistor M1 is biased close to threshold voltage V_{th}, which allows exploiting nonlinearities for the purpose of half-wave rectification of the RF input signal. Capacitance C1 and circuit Z3 both act as the low-pass filter, which is required for envelope and thus AM detection.

 DOI: 10.1109/ESSCIRC.2016.7598247.

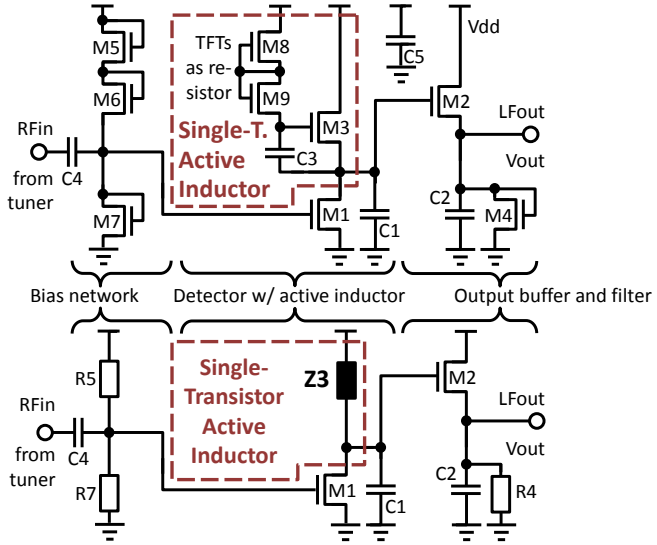

Fig. 2. Full schematic of AM detector circuit with active inductor load (top) and simplified schematic of the same AM detector circuit (bottom).

TABLE I. DIMENSIONS AND VALUES OF THE ELEMENTS OF AM DETECTOR CIRCUIT AND THE EQUIVALENT CIRCUITS FOR ACTIVE INDUCTOR Z3.

TFT	W/L in µm/µm	Ele-ment	Value	Ele-ment	Value
M1	200/5	C1	11 pF	Cgd3	0.85 pF
M2	300/7	C2	70 pF	gm3	5.2 µS
M3	50/25	C3	269 pF	rds3	3.0 MΩ
M4	50/30	R4	10 MΩ[a]	R8	20 MΩ[a]
M5, M6	40/50	R5	2x24 MΩ[a]	C8	0.33 pF
M7	190/13	R7	5 MΩ[a]	C3p	1.18 pF
M8	40/60	C4	296 pF	L3s	1060 H
M9	40/5	C5	840 pF	R3s	195 kΩ
		Vdd	5 V	R3b	2.52 MΩ

[a] Value is based on a dedicated measurement datum specific to operating point within the circuit.

B. *Single-Transistor Active Inductor*

The innovative realization of the single-ended active inductor circuit Z3 (Fig. 2) is the key to enabling the exceptional performance of the presented AM detector circuit. The active inductor uses only one active transistor M1, has a low complexity, and requires a small chip area of only 0.37 mm². Its largest component is capacitor C3. Transistors M8 and M9 solely serve as resistive elements.

Fig. 3 and Table I show small signal equivalent circuits for Z3. All of them match the comprehensive simulation of subcircuit Z3 (consisting of M3, M8, M9, and C3) using Shur's TFT model [8], which we fitted to this technology. The impedance of Z3 is plotted in Fig. 4. From these plots it can be seen that Z3 behaves like an active inductor, i.e. a parallel tank circuit. It is highly inductive (L3s=1060 H) for frequencies below f_0=4.7 kHz. This is desired as it enables setting the operating point of TFT M1, while exhibiting a very high resistance and thus enabling a very high voltage gain of the CS stage between the lower and upper cutoff frequencies of $f_{gr,l}$=400 Hz and $f_{gr,u}$=50.0 kHz. In this frequency range the Q-factor Qs(f) of series elements L3s+R3s ranges from 14 to 1710. Fig. 5 shows this Qs(f) as well as the small signal

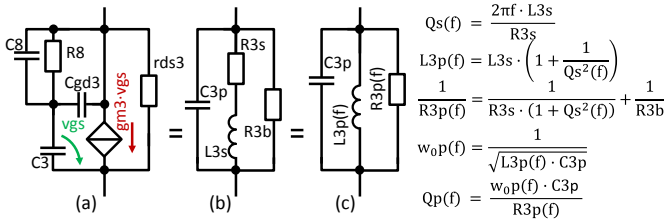

Fig. 3. Small signal equivalent circuits for the active inductor Z3. Note that elements L3p and R3p of circuit (c) dependend on frequency f. They can be caluclated based on the elements of circuit (b) as shown.

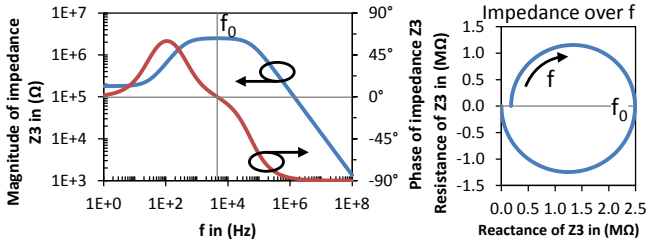

Fig. 4. Impedance of active inductor Z3. The magnitude of the impedance peaks at f_0=4.7 kHz and has a -3dB-bandwidth (BW) of 54.6 kHz.

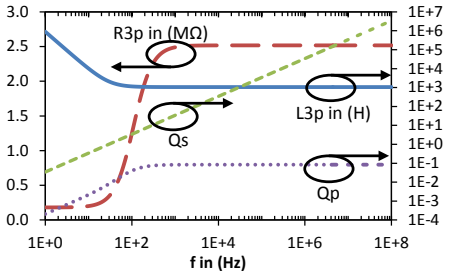

Fig. 5. Parameters of small signal equivalent tank circuit Fig. 3 (c) for Z3.

parameters and the Q-factor Qp(f) for the equivalent parallel tank circuit shown in Fig. 3 (c). It can be seen that the Q-factor of the parallel tank circuit is only 0.084, which is equivalent to its wide relative bandwidth, and is required in this work to achieve the targeted baseband frequency range.

To realize the required small lower cutoff frequency $f_{gr,l}$ a very high resistance R8 has to be implemented. As mentioned above, no dedicated resistance layer is available in this technology. Therefore we implement R8 using the scheme of oppositely stacked MOS diodes [9] with TFTs M8 and M9.

To fundamentally improve the highest gain achievable by the CS stage loaded with active inductor Z3, the ratio $|Z3(f_0)|/|Z3(f=0)|$ would have to be increased. This would allow a larger load resistance and thus higher gain in the baseband frequency range, while maintaining the same operating point. However, the above impedance ratio is defined by the intrinsic gain $g_m \cdot r_{ds}$ of the TFT technology.

C. *Bias Network and Output Buffer*

The high input impedance (4.5 MΩ || 3.5 pF) of the bias network M5, M6, and M7 (or equivalently R5 and R7, see Fig. 1 and Table I) allows connecting the AM detector directly to a tuned antenna, without the need for an additional RF amplifier, provided that the received signal is strong enough. This is for example the case for short range applications like RFID. Furthermore, the channel width of bias TFT M7 is chosen to be almost identical to that of active TFT M1, because this leads to a strong robustness of the CS stage against threshold voltage variations.

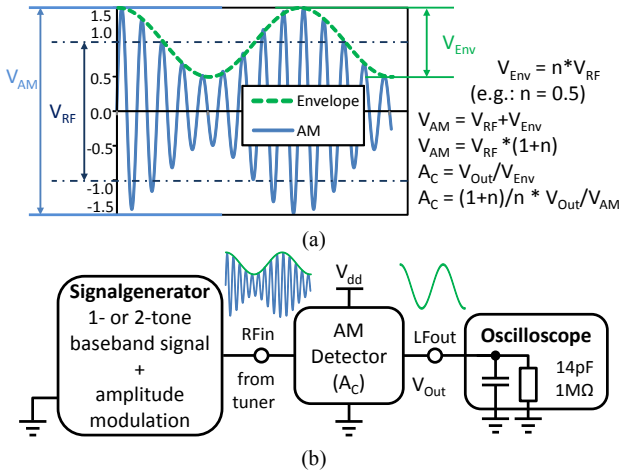

Fig. 6. (a) Definition of voltage conversion gain A_C used in this work. The modulation index n is n=50% in this example. (b) Measurement setup.

The output is driven by a source follower buffer stage (M2), which also serves as a low pass filter for further carrier suppression. This low pass filter consists of C2 || R4 || Zload, i.e. the corner frequency depends on the load condition. The expected load impedance Zload of the to-be connected limiting amplifier (see Fig. 1) is in the order of 1 MΩ || 80 pF. For easy characterization under similar load conditions, we intentionally connect the increased integrated capacitor C2. For the measurement setup shown in Fig. 6 the expected corner frequency of the output low pass filter is 19 kHz. When the AM detector circuit is actually integrated in the OOK receiver module, capacitor C2 can be disconnected. Fig. 7 shows the die photograph of the AM detector circuit. It can be seen that C2 is laid-out in four segments, which can be disconnected individually by scratching interconnect with a sharp needle. This allows tuning the corner frequency of the output low pass filter.

IV. Measurements and Comparison

A. Measurement Setup

All measurements were performed with an input signal of carrier frequency f_c, amplitude modulated by one or two baseband tones f_{bb} and f_{bb2}. The definitions for the signal amplitudes, modulation index n, and voltage conversion gain A_C are given in Fig. 6 (a). The output of the AM detector circuit was monitored with an oscilloscope. During two tone measurements the FFT of the acquired time domain signal V_{Out} was calculated by the oscilloscope. Fig. 6 (b) shows the measurement setup.

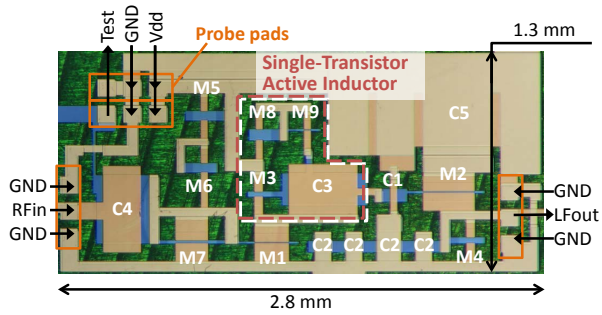

Fig. 7. Die photograph of the AM detector with single-transistor active inductor.

B. Measurement Results

The AM detector circuit can operate on a supply voltage V_{dd} in the range from 4 V to 6 V. All results are presented for V_{dd}=5.0 V. The supply current I_d for the default input parameters (see Fig. 9), which lead to a conversion gain of A_C=19.2 dB, is I_d=78µA, i.e. the power consumption of the AM detector circuit is P=0.39 mW. During all measurements the internal capacitance C2=70 pF was connected to imitate the expected load conditions that will be caused by the to-be connected limiting amplifier (see Fig. 1 and Sec. III-C).

Fig. 10 shows the input and output waveform for the default values of the measurement parameter set (f_c, f_{bb}, V_{AM}, and n, see Fig. 9). Fig. 8 plots A_C over input amplitude V_{AM}. Fig. 9 shows the conversion gain A_C over carrier frequency f_c, base band frequency f_{bb}, and modulation index n, for two different input amplitudes V_{AM}. As expected, an expansion characteristic can be observed in Figs. 8 and 9 (c) before clipping occurs. The result in Fig. 9 (a) shows that the -3dB-bandwidth of the carrier frequency f_c is in the order of 7.5 MHz and that A_C drops to 6 dB at around f_c=22 MHz. In the ISM band at 13.56 MHz gain A_C is 11.6 dB.

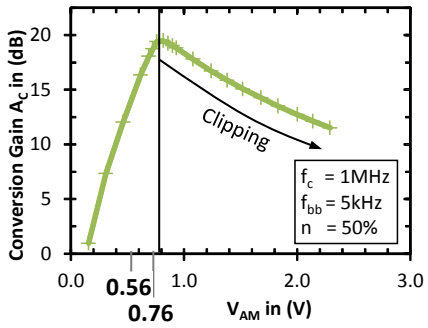

Fig. 8. Measurements of conversion gain over input peak-to-peak amplitude.

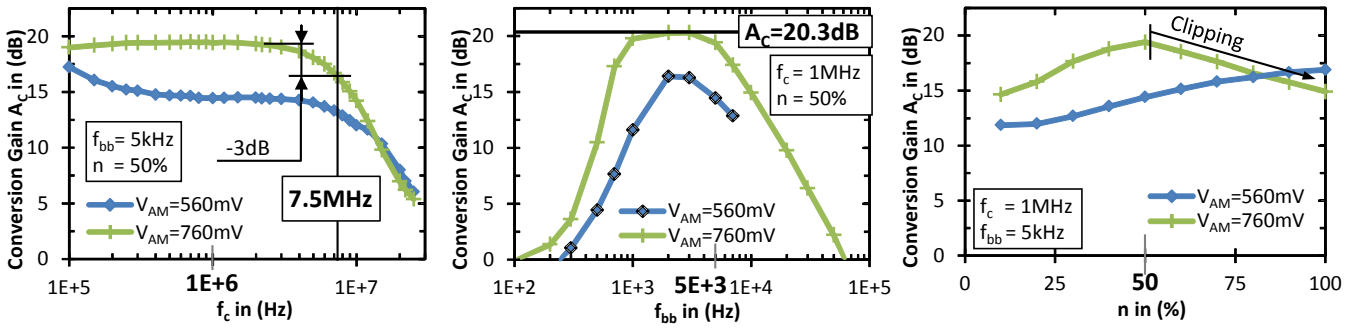

Fig. 9. Measurements of conversion gain over f_c, f_{bb}, and n. The default input parameter values are f_c=1 MHz, f_{bb}=5 kHz, and n=50%.

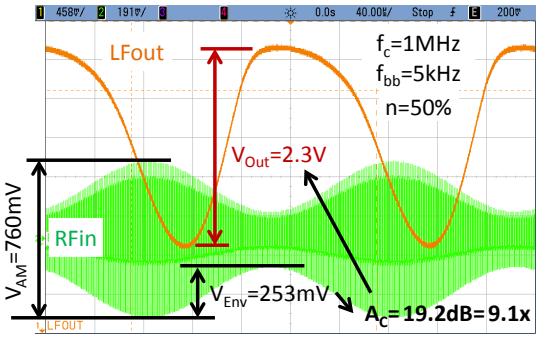

Fig. 10. Screen shot of input waveform RFin and output waveform LFout for the default values of the measurment parameter set (also listed in Fig. 9).

The baseband frequency response shown in Fig. 9 (b) is close to the prediction in Sec. III. It is dominated by the characteristics of the active inductor subcircuit Z3 for frequencies below f_{bb}=10 kHz. Above f_{bb}=10 kHz the output low pass filter causes the roll off (predicted cutoff was at f_{bb}=19 kHz). The highest conversion gain of A_C=20.3 dB is observed between f_{bb}=2 kHz and 3 kHz. In simulation the highest resistance of Z3 and thus highest gain was predicted for f_{bb}=4.7 kHz. Concluding, Fig. 9 (b) shows that the detector circuit covers a baseband frequency range from about 600 Hz to 10 kHz, which allows its use for the target low data rate OOK wireless communication application in a smart label. It also covers most of the frequency range for voice applications (typically 300 Hz to 3.4 kHz).

Linearity is not a primary design goal for this AM detector, since its intended usage is for digital OOK data communications. Still, we successfully conducted two tone measurements for input tones f_{bb}=900 Hz and f_{bb2}=1 kHz. For this measurement the modulation index was swept from 0 % to 50 %, while the input carrier signal amplitude V_{RF}=238 mV was constant. The extrapolated IIP3 and OIP3 are $V_{Env\ RMS}$= -17 dBV and $V_{Out\ RMS}$ = -8.5 dBV, respectively.

C. Comparison

Table II compares the presented AM detector circuit to previous works based on TFT technology. It is significantly smaller (1.6x), consumes 9-times less power than previous a-IGZO based circuits and provides 1.8x higher conversion gain. The carrier frequency ranges given in Table II for this work and [4] are based on -3dB-bandwidths, while for [9] an upper limit of 20 MHz is given. The conversion gain of our work is 7 dB at f_c=20MHz, while [9] achieves about 17 dB at the same frequency. However the conversion gain of [9] is outperformed by our work for f_c<9 MHz. Results provided for [11] are for the ISM band at 13.56 MHz. The conversion gain at 13.56 MHz of our work is 11.6 dB (3.8x) and thus exceeds that of [11].

V. Conclusion

In this work we presented an AM detector circuit in a fully bendable a-IGZO TFT technology. It improves over previous TFT based works regarding gain (1.8x), chip area (1.6x), and power consumption (9x for a-IGZO based circuits). Key element for this improvement is the innovative realization of a single-ended single-transistor active inductor in TFT technology. The AM detector circuit can be used for wireless data communications, for example for RFID or smart labels, where it can increase the sensitivity and range compared to passive solutions. Beneficial to such applications, it has a low power consumption and can be connected directly to a tuned antenna, without an additional RF amplifier, because of its high input impedance and conversion gain.

TABLE II. Characteristics and comparison to previously published AM / envelope detectors based on TFT technology.

	This work	**[5]**	**[9]**	**[10]**	**[11]**
Technology	a-IGZO TFT	a-IGZO TFT	a-IGZO TFT	a-Si TFT	C-OTFT
Supply voltage Vdd	5 V	5 V	5 V	20 V	40 V
Baseband frequency range	600 Hz – 10 kHz	< 100 Hz – 8 kHz	400 Hz – 10 kHz	2 kHz	75 Hz
Carrier frequency range	100 kHz – 7.5 MHz	100 kHz – 1 MHz	1 MHz – 20 MHz	900 kHz	13.56 MHz
Conversion gain Ac	20.3 dB (10.3x)	10.1 dB (3.2x)	15.3 dB (5.8x)		ca. 3.5 dB (ca. 1.5x)
Power consumption	0.39 mW	3.5 mW	36 mW	< 2.2mW	0.32 mW
Transistors	9	7	24		7
Stages (w/o buffer)	1	2	5	1	1
Chip core area	3.6 mm²	5.7 mm²	26.85 mm²		280.0 mm²

Acknowledgments

This work was supported in part by the European Commission under project FLEXIBILITY under Grant 287568, in part by the German Research Foundation within the Cluster of Excellence "Center for Advancing Electronics Dresden-Organic Path", and in part by the DFG (Deutsche Forschungsgemeinschaft), within the project "Low-Voltage High-Frequency Vertical Organic Transistors" as well as WISDOM and the Coordination Funds of SPP 1796.

References

[1] G. A. Salvatore et al., "High performance flexible electronics for biomedical devices", Engineering in Medicine and Biology Society (EMBC), pp. 4176-4179, 2014.

[2] N. Münzenrieder et al., "Contact resistance and overlapping capacitance in flexible sub-micron long oxide thin-film transistors for above 100 MHz operation", Applied Physics Letters 105, 263504, 2014.

[3] K. Nomura, et al., "Room-temperature fabrication of transparent flexible thin-film transistors using amorphous oxide semiconductors," Nature 432, pp. 488-492, 2004.

[4] T. Meister et al., "3.5mW 1MHz AM detector and digitally-controlled tuner in a-IGZO TFT for wireless communication in a fully integrated flexible system for audio bag", Symp. on VLSI Circuits 2016, in press.

[5] T. Meister et al. "Textile loop antenna and TFT channel-select circuit for fully bendable TFT receivers", International Microwave and Optoelectronics Conference (IMOC), pp. 1-5, 2015

[6] R. Shabanpour et al. "A 2.62 MHz 762 µW cascode amplifier in flexible a-IGZO thin-film technology for textile and wearable-electronics applications", Int. Semiconductor Conference Dresden-Grenoble (ISCDG), pp. 1-4, 2013.

[7] R. Shabanpour et al., "Cherry-hooper amplifiers with 33 dB gain at 400 kHz BW and 10 dB gain at 3.5 MHz BW in flexible self-aligned a-IGZO TFT technology", Intelligent Signal Processing and Communication Systems (ISPACS), pp. 271-274, 2014.

[8] M. S. Shur, H. C. Slade, M. D. Jacunski, A. A. Owusu, and T. Ytterdal, "SPICE models for amorphous silicon and polysilicon thin film transistors", J. Electrochem. Soc., 144(8), pp. 2833-2839, 1997.

[9] K. Ishida et al., "15 dB conversion gain, 20 MHz carrier frequency AM receiver in flexible a-IGZO TFT technology with textile antennas", Symp. on VLSI Technology, pp. C194-C195, 2015.

[10] L. Huang et al., "A super-regenerative radio on plastic based on thin-film transistors and antennas on large flexible sheets for distributed communication links", ISSCC, pp.458-459, 2013.

[11] V. Fiore et al.,"A 13.56MHz RFID tag with active envelope detection in an organic complementary TFT technology", ISSCC, pp. 492-493, 2014.